AIAA 2001-0838
Tunnel and Natural Icing Tests of a Helicopter Engine Cooling Bay Inlet

K. Al-Khalil and E. Irani
Cox & Company, Inc.
New York, NY 10014
D. Rowley
GKN Westland Helicopters
Yeovil, UK

39th Aerospace Sciences Meeting & Exhibit
8 - 12 January 2001
Reno, Nevada

TUNNEL AND NATURAL ICING TESTS OF A HELICOPTER ENGINE COOLING BAY INLET

Kamel Al-Khalil, Ph.D.*, Eddie Irani, Ph.D.†
Cox & Company, Inc., New York, NY 10014

Dave Rowley‡
GKN Westland Helicopters, Yeovil, UK

ABSTRACT

A program was undertaken to design a thermal anti-icing system for engine cooling bay inlets (scoops) of a tri-engine helicopter. The three scoops are located downstream of each engine main air intake. The development of the anti-icing system was conducted mainly during a one-month test program in an indoor icing wind tunnel. Subsequently, flight test units were produced and configured with corresponding heated surfaces and instrumentation for a full winter season test in natural icing conditions. The ice protection system's performance during the flight trials was fully evaporative as designed. Also, very good correlations were obtained between the flight and the tunnel experimental data.

1.0 SUMMARY

Flight in icing conditions can jeopardize the safety of the crew and passengers as well as the aircraft. Generally, ice protection systems are employed to overcome the detrimental effects of such conditions. Historically, certification of rotorcraft for flight into known icing conditions has been very limited as a result of added challenges compared to fixed wing aircraft. These challenges are a result of the complexity of the airflow and the associated systems of concern, as well as the operational characteristics of helicopters.

This paper is concerned with the ice protection systems of the engine cooling bay scoops on the GKN Westland Helicopter EH101, shown in Figure 1. The aircraft is equipped with three engines: the No. 1 (Port) and the No. 3 (Starboard) are located symmetrically upfront, and the No. 2 (Center) is located on the left side of the aircraft, behind the No. 1 engine. There corresponds one scoop to each engine, the No. 1 and the No. 3 being identical. Reference to Scoops 1 and 3 will made interchangeably. Figure 1 shows the location of these scoops on the Helicopter. The scoops are mounted on the side of the aircraft cowling, downstream of each engine, to allow ram air into the bay for the purpose of cooling the engine. An engine-driven ejector controls the inlet airflow rate through each scoop.

*Manager, LIRL Icing Wind Tunnel, Senior Member AIAA
†Aerospace Research Engineer, Member AIAA
‡Principal Engineer, Member AIAA

Earlier flight tests proved that the scoops would collect ice during flight in icing conditions. A de-icing system was deemed unacceptable as ice shed could impact on, and damage the tail rotor, which would jeopardize flight safety. A fully evaporative system was then selected to eliminate the probability of runback ice formation. Each scoop incorporates integral ice protection heating elements, and is connected to, and operated by, a dedicated control unit.

Tunnel and flight tests of the Scoops Ice Protection System (SIPS) were conducted. Development of the evaporative SIPS was performed in the Icing Wind Tunnel (IWT) at the Cox LeClerc Icing Research Laboratory (LIRL) shown in Figure 2. Tunnel data were analyzed and final SIPS design configuration was obtained for each of the scoops. Prototype units, shown in Figure 3, were fabricated with instrumentation and mounted on a flight test aircraft for a full winter season of testing in natural icing conditions. The red color in Figure 3 indicates location of engine fire extinguisher access and not the heater location. The flight test operation was based in Halifax, Nova Scotia, Canada.

2.0 TUNNEL SETUP VALIDATION CRITERIA

To validate the test setups, ice was accreted separately on both Scoop 1 and Scoop 2 in an attempt match the ice shapes obtained during previous EH101 natural icing trials. These accretions were for both glaze and rime conditions. Air mass flowrate into the scoops was generally set to a maximum value 1.6 lb/sec for Scoop 1 and Scoop 3, and 2.8 lb/sec for Scoop 2.

The time-averaged operating conditions for the two considered flights are:

Flight 266 (glaze):

TAS = 117 Kts
OAT = - 4.3 °C (24 °F)
LWC = 0.18 g/m^3
MVD = 10 microns
Time = 97 minutes

Flight 257 (rime):

TAS = 122 Kts
OAT = - 15.7 °C (4 °F)
LWC = 0.10 g/m^3
MVD = 11 microns
Time = 96 minutes

The low values of LWC encountered in flight cannot be reproduced accurately in the IWT. To account for this, the LWC in the tunnel was scaled up and the exposure time was scaled down by the same factor to produce the equivalent accretion. The lowest attainable and controllable LWC of 0.32 g/m^3 was used.

3.0 TUNNEL TEST FIXTURES

The IWT in the LIRL facility [1], shown in Figure 2, can simulate airspeeds in excess of 200 mph at temperatures below –22 °F (–30 °C) in its upstream Test Section-1. This section measures 28 inches wide by 46 inches high by 6.5 ft long. The tunnel has a diffuser expanding linearly between this main test section and the larger (48”x48”) Test Section-2 downstream. All tests were conducted on a full-scale model of each scoop mounted in the modified Test Section-2 as described in paragraphs 3.1 and 3.2.

Tunnel testing of each scoop was conducted in two phases:

(a) Qualification of the setup:

This consisted of demonstrating that the setup appropriately duplicates the aerodynamics of actual installations. In addition, it was demonstrated that the setup closely reproduces ice shapes --therefore impingement-- observed under certain flight conditions for which actual flight photographs from previous icing trials existed.

(b) Heater development tests:

A set of scoops was fabricated with integral heating elements. The heaters were divided into multiple individually controlled zones to yield an optimum power distribution for the anti-icing system design.

3.1 Scoop No. 1 Test Setup:

The test setup of Scoops 1 and 2 were different as a result of their unique sizes, locations on the aircraft, and ice accretion shapes. Figure 4 is a side view image of the Scoop 1 setup on a modified tunnel ceiling. A ramp was formed on the ceiling following an angle to reproduce actual local airflow. The resulting scoop location was about 1 foot below the original ceiling. The added blockage also allowed a full airspeed of 120 KTAS to be simulated in Test Section-2. The scoop air inlet is connected through a plenum to the tunnel scavenger system to simulate the correct flow rate through the engine bay.

The validation procedure described in paragraph 2.0 was used successfully in the setup and validation tests for Scoop 1. For this scoop, an icing bar was also used to calibrate accretion in the vicinity of the scoop as shown in Figure 5. This figure also shows the cloud uniformity in the vicinity of the scoop. The LWC deficiency near the sidewalls has no impact on the scoop. It is a result of the lateral expansion in the diffuser section between the two test sections. Vertical cloud uniformity is closely maintained near the scoop.

Photographs of ice accretion on the forward Scoop 1 and Scoop 3 during the two flights chosen for the validation are illustrated in Figures 6 and 7. These correspond to the glaze and rime icing conditions, respectively. The corresponding ice shapes produced in the tunnel are shown in Figures 8 and 9 for the glaze condition, and Figure 10 for the rime condition.

The main difference is the additional ice accretion obtained on the side buttresses in the tunnel versus the flight tests. The reason is that the current scoop geometry tested in the tunnel has front facing buttresses, which are at steeper angles relative to the freestream. The earlier version of Scoops 1 and 3 had buttresses that extended further upstream at a shallower angle relative to the freestream. However, both versions had exactly the same geometry near the centerline. Figure 9 shows the cross section of the ice accreted in the tunnel, which compares well with the corresponding flight ice shape shown in Figure 6 during glaze conditions. Also, Figure 10 shows that the ice thickness accreted on the hi-lite is nearly 1.1 inches which is very close to that observed during the rime condition of Flight 257 as seen in Figure 7.

3.2 Scoop No. 2 Test Setup

The test setup for Scoop 2 was more elaborate and challenging than that of Scoop 1. As mentioned earlier, the criteria for the validation of the setup requires matching the local flow as well as ice shapes from earlier flights. These ice shapes are shown in Figures 11 and 12 for the glaze and rime conditions, respectively. Clearly, the uneven ice shape distribution around the scoop hi-lite could not be simulated with the setup of Scoop 1. The following paragraphs describe the different attempts to correctly simulate the flight conditions.

3.2.1 Full Scale Fairing

Due to the complexity of the airflow in the neighborhood of Scoop 2, it was considered necessary to simulate portions of the actual aircraft contours in the tunnel. A decision was made that the primary method of flow simulation was to utilize a full-scale aircraft fairing from the EH-101 upper deck, which encompasses Engine 1 and Scoop 1.

The fairing was mounted to the tunnel sidewall adjacent to the ceiling within diffuser No.1 downstream of Test Section-1, and extended partially into Test Section-2 as shown in Figures 13 and 14. The fairing contours matched that of the ramp and the lowered ceiling when mounted. Figure 14 illustrates the front view of this setup, which gives an indication of the blockage.

The upstream section was a ramp, which followed the cutout in the full-scale fairing, down to about 12 inches below the tunnel ceiling. At this point, it blended into a horizontal fixture/ceiling that ran to the back of Test Section-2. Scoop 2 was attached to this modified horizontal ceiling.

One of the clear disadvantages of this fairing was its relatively high blockage to the flow in the tunnel. Testing showed that little to no ice accreted on the fairing surface as a result of its good aerodynamic shape. The fairing resulted in an ice shape on Scoop 2 that was tapered in thickness as shown in Figure 15. Comparing that to Figure 11, the experimental ice shape was the reverse of that in flight. Basically, the fairing shadowed a portion of the scoop surface and produced a higher cloud density on the opposite side.

Prior to removing the fairing from the tunnel, a flow visualization test was conducted to investigate the flow angularity in the vicinity of the scoop. Tufts were used for this purpose as shown in Figure 16. The left side in this figure, which corresponds to the bottom side on the aircraft, had higher flow angularities than the right side. These angles were also verified using a 3D Navier-Stokes CFD solver.

3.2.2 Nozzle Allocation & Flow Deflector

A fall back plan was considered prudent in case the full scale fairing setup was unable to produce the ice shapes, as was the case, rendered during the earlier natural icing trials. The setup is similar to the one used for Scoop 1 with two exceptions: (1) the nozzles on the spray bars were relocated to produce high cloud water concentration on the lower side of Scoop 2 as observed during the flight trials; and, (2) the ramp consisted of two sections as with the fairing setup. The upstream section consisted of a ramp, and the downstream horizontal section held the scoop.

The resulting ice accretions looked nearly like those in the icing trials. Nevertheless, even though the ice thickness was similar, the actual flight scoop had the flow approaching at an angle on the lower side. To produce that local flow feature, a small airfoil flow deflector was installed near the scoop as shown in Figures 17 and 18. Comparison of Figure 18 to Figure 19 verifies the proper simulation of the local aerodynamic flow.

Furthermore, the nozzle allocation on the spray bars was adjusted to optimize the ice accretion and Liquid Water Content (LWC). The resulting ice shape is shown in Figure 19, which compares well to the actual flight ice shape shown in Figure 11. This setup was used as the final configuration for Scoop 2 tunnel testing during the SIPS heater development.

4.0 DATA ACQUISITION AND CONTROL

Tunnel tests were conducted on a full-scale model of each scoop. An electro-thermal anti-icing system was designed and integrated into the scoops. The heaters used on the test models were divided into multiple separately controlled zones. Each zone had one RTD thermal sensor and one type-T thermocouple. The instrumentation permitted temperature and heat flux data to be recorded and displayed at one-second intervals during the test.

The Cox Thermal Test Management System (TTMS) was used to power the models and record the data. The TTMS is a computer based test management and data acquisition system. Power was regulated to each particular zone based on either constant temperature or constant power using the TTMS. Usually, a set point temperature is used and the power was adjusted accordingly. In most normal operating conditions at sub-freezing temperature and full airspeed of 120 KTAS, several of the heaters were operating at 100% duty cycle with the corresponding sensor temperature being below the set point. The power density in each zone was optimized for fully evaporative performance, and not necessarily for constant temperature.

5.0 ICING TUNNEL TESTS

The engine bay inlet SIPS was designed to operate as a fully evaporative system. It meets several airworthiness requirements that adhere to the following regulations:

(ii) British DEF STAN 00-970 Chapter 711
(iii) US FAR 29.1419
(iv) European JAR 29.1419

Testing was conducted at various environmental conditions. Table 1 lists an abbreviated version of the test and design conditions.

Table 1: Abbreviated list of icing conditions

Condition	OAT EC	LWC g/m^3	Duration minutes	VMD microns
I Continuous Maximum Icing	0 -10 -20 -30	0.8 0.6 0.3 0.2	Unlimited	15-20
II (A) Periodic Maximum Icing	0 -10 -20 -30	1.2 0.90 0.45 0.30	15 minutes	15-20
II (B) Intermittent Icing	0 -10 -20	1.50 1.35 1.20	5 minutes	15-20

The effect of mixed icing conditions on the power requirements of evaporative anti-icing systems has been addressed in Reference [2]. The report demonstrates that the power required for evaporative systems is a strong function of the total water content (liquid and ice crystals). In evaporative systems, conditions of high LWC are more severe than the mixed phase conditions which have less total water content.

5.1 Scoop 1 Thermal Tests

The tunnel SIPS development program was involved with numerous studies. This paper will provide a summary of a select number of test points. Table 2 provides a cross-reference for some of the icing conditions and corresponding figure numbers for Scoop 1 discussed in this document.

Table 2: Selected icing conditions for Scoop 1

Test Point	Fig. No.	V KTAS	OAT °F	LWC g/m^3	MVD µm
1	20	120	23	1.0	18
2	21	120	-4	0.45	18
3	22	120	-5	0.6/0.9	18
4	23	120	14	0.6/0.9	20
5	24	120	23	0.8	35
6	25	120	14	0.0/1.35	18

Test Point 1 (Figure 20)

This is a warm condition conducted at a very high and continuous LWC. Minor runback was observed on the bottom of the front buttress surfaces near the flange. As a result of the local flow reversal at those locations, the runback was seen to flow a small distance forward and then back downstream. However, no frozen runback was observed. Surface wetness extended about 0.5 inch beyond the direct impingement area.

The scoops mount to the aircraft composite structure, which led to a design temperature limit on the scoop flange interface of 90 °C (194 °F) or less. The scoop structure is made of cast aluminum which has a high thermal conductivity. Consequently, the heaters were offset from the flange by about 0.5 inch or more. This reduced the anti-icing system performance on the front facing surfaces near the flange. A thermocouple was installed on the flange near the front facing buttress where the heater power density is high. The measured temperature at this location was 60 °F in this case, which is within the acceptable limit.

Test Point 2 (Figure 21)

This is a relatively cold condition case. Several helpful observations were made during this run. The flange was at about 25 °F most of the time. Little ice was observed to form on the buttress near the flange. This is a direct result of the fact that the bottom 0.5 inch of the buttresses was unheated.

Another observation made was the ice growing forward (into the air stream) on the forward facing step of the flange upstream of the buttresses. This phenomenon is thought to be attributable to the common tunnel wall icing effects due to the turbulent flow. The photographic data from the earlier icing trials did not show ice growth on the bottom of the buttresses. However, the buttress heaters were extended towards the flange in the follow-up prototype flight scoops.

Test Point 3 (Figure 22)

This case is a Continuous Maximum (CM) icing condition with periodic incursions into Periodic Maximum (PM) icing conditions at a warm temperature and high LWC as required by the British DEF STAN. The PM conditions extend 6 Km (3.24 N.M.) horizontally. Despite the relatively cold temperatures, the scoop remained clear of any ice formation for the entire duration as shown in Figure 22. Surface wetness was observed to be limited to slightly past the direct impingement area.

Test Point 4 (Figure 23)

This is a repeat of Test Point 3 but at a warmer condition. The flange temperature averaged +57 °F in the initial dry condition and +38 °F in the wet conditions.

The runback extended slightly beyond the direct impingement during the high LWC exposure of the Periodic Maximum conditions. There was no ice accumulation on the scoop surface except on the forward facing step of the flange. Again, this could be explained as being an artificial icing tunnel effect due to the flow turbulence.

Test Point 5 (Figures 24)

In this case, the effect of large droplets on the anti-icing system performance is evaluated. A size of 35 microns MVD was selected with a higher than nominal LWC. The nozzles produce droplet distributions having a spectrum that extends further towards larger droplets than would the equivalent MVD size in a Langmuir-D distribution. Consequently, the impingement limits obtained in the tunnel are conservative.

It was clear from Figure 24 that the impingement zone was extended. The runback was observed to be as far as one to 1.5 inches beyond the direct impingement limits. A small amount of runback was observed near the flange of the forward facing buttresses. This is consistent with previous observations. The flange temperature was about 57 °F.

Test Point 6 (Figure 25)

This is an Intermittent Maximum Icing condition defined here as a continuous condition in dry air with periodic incursions in high LWC clouds extending 2.6 N.M. horizontal. This corresponds to 1.3 minute wet cycles at 120 Kts. This condition complies with FAR-29C requirements with 10,000 ft altitude limitations.

During these intermittent conditions, some runback was observed several inches downstream of the direct impingement region. However, the surface was still heated at those locations. Following each wet cycle, all runback water was cleared within less than 10 seconds.

5.2 Scoop 2 Thermal Tests

The setup of Scoop 2 was more complicated and time consuming than Scoop 1 setup. However, the anti-icing system development was less challenging for two reasons: (1) ice collection efficiency was less than half of Scoop 1 which meant that lower power densities were required, and (2) lessons were learned from Scoop 1 since its SIPS development occurred first.

Based on the relatively cool temperatures at the flange, and the accretions observed near the bottom of the buttresses, the corresponding heaters were extended closer to the flange. Despite believing that tunnel turbulence was to blame for this artifact, this action was taken to insure a successful flight test and reduce risks, which would greatly impact the overall program schedule.

Table 3 provides a cross-reference for some of the icing conditions and corresponding figure numbers for Scoop 2 discussed in this document.

Table 3: Selected icing conditions for Scoop 2

Test Point	Fig. No.	V KTAS	OAT °F	LWC g/m^3	MVD µm
7	26	120	23	0.0/1.43	18
8	27	60	16	1.74	16
9	28	120	-22	0.0/1.2	18

Test Point 7 (Figure 26)

This is an Intermittent Maximum Icing condition defined here as a continuous condition in dry air with periodic incursions in high LWC clouds, similar to Test Point 6 of Scoop 1.

Three complete cycles were executed. During each wet cycle, a small amount of water was observed on the hi-lite and the lower sides of the buttresses, but there was no runback. Following each cycle, the scoop was clear of any runback and dry within 3 seconds of shutting off the cloud spray.

Test Point 8 (Figure 27)

The purpose of this run was to determine the effect of airspeed, 60 Kts in this case, on the SIPS anti-icing performance. The minimum tunnel calibrated LWC condition was used. Because of the low airspeed, the LWC was 1.74 g/m^3. Despite this high LWC, the system performance was fully evaporative as shown in Figure 27 with no visible moisture on the surface.

Test Point 9 (Figure 28)

Four full cycles of Intermittent Maximum condition were executed at the coldest temperature of –22 °F (-30 °C) in the test matrix. This particular Test Point turned out to be the determining design condition for Scoop 2.

Due to the high LWC condition (1.2 g/m^3) at an extreme cold temperature, some runback was seen beyond the heated zone in the direct impingement region. This is on the buttress side with the higher water catch as shown in Figures 11 and 19. The heater powers were as determined in the previous runs.

To remedy this problem, downstream heaters had to be activated with the rest of the heaters in the direct impingement zone. This required heating a large surface area. The trade-off is to increase the power density in the direct impingement zone and fully evaporate the water to prevent any runback flow to unheated downstream regions.

The proper design method is the one that yields the minimum power requirements while insuring that operating temperatures are within the material limits. The heating efficiency in aft areas is below 30% because the water runs back as individual rivulets instead of as a liquid film. This reduced wetness factor downstream, coupled with a large surface area, would have required a large amount of power to evaporate the runback water. Instead, adjustments were made to the heater powers within the impingement zone to evaporate all the water as it impacts the surface. Consequently, formation of runback was eliminated even in the cases of the Periodic and Intermittent Max with their high LWC conditions.

6.0 NATURAL ICING FLIGHT TESTS

The EH101 Helicopter icing trial tests occurred during the 1999-2000 winter season. The flight test program was based in Halifax, Nova Scotia in Canada. Testing extended to mid April of 2000.

Following the icing development tests in the Cox IWT, the data were analyzed and a final design for each scoop was chosen to meet all the requirements. A set of scoops with integral ice protection system was manufactured based on the final design. The scoops were mounted on a flight test aircraft for validation and qualification of the system performance in natural icing conditions.

Each of the final design scoops was instrumented with five type-T thermocouples for data acquisition during the flight tests. The first thermocouple was located on the radius between the scoop flange and the buttress heaters. Placing this thermocouple directly on the backside of the flange was not practical since the scoops had to be secured flush to the aircraft structure, and this would damage the thermocouple assembly.

Generally, the thermocouples were centered behind certain key heater segments. Each of these segments operated at a different power density (W/in^2). Scoop 3 is identical by design to Scoop 1 as a result of geometric symmetry, and the assumed flowfield symmetry. However, as will be shown, Scoop 3 usually runs a little cooler than Scoop 1 in flight.

The test aircraft was heavily instrumented for flight conditions including: altitude, airspeed, outside air temperature, LWC, and MVD. Numerous other instruments not related to the current topic are not listed. Power to the heaters was controlled based on feedback from sensors strategically located within the heater lay-up. Due to the requirements for an evaporative ice protection system performance, some of the heaters operated at high power densities ranging from 35 to 42 W/in^2. The heater construction is capable of operating continuously at over 400 °F (204°C). However, the heaters operated at or below 325 °F (163 °C) with a 100% duty cycle in most cases.

7.0 COMPARISON OF TUNNEL AND FLIGHT DATA

In order to compare flight data to tunnel data, many of the variables had to match between the two conditions. Some of the important variables are airspeed, ambient temperature, and LWC. There were enough dry data from flight to compare to tunnel data. It was difficult to find a wet condition where the LWC is large enough and sustained for several minutes. However, it was seen from tunnel testing that close to steady state is achieved in less than one minute when LWC conditions are periodically varied (e.g. Periodic Max and Intermittent Max conditions). Therefore, flight conditions were selected where the variations within at least 2 minutes were small and an average value was used to represent the actual flight condition.

For comparison purposes, Tables 4 and 5 summarize flight (FLT) and corresponding tunnel (RUN) conditions for Scoop 1 and Scoop 2, respectively. Inflight data for Scoop 3 are also included with those of the identical Scoop 1 in the comparisons.

Figure 29 shows results of flight into dry air conditions for Scoops 1 and 3, compared to dry tunnel data. There is some variability within the flight data itself from flight to flight and between Scoop 1 and Scoop 3. With this in mind, the tunnel data (dark color) compares well with the flight data. It should be mentioned that the flange temperature TC1 was warmer in flight because the buttress heaters were extended closer to the flange in the flight units as a result of the tunnel observations of ice accretion close to the flange. However, flight video did not show that ice accreted close to the flange. This was suspected as tunnel turbulence may have caused the additional impingement. Also, TC5 was warmer in the tunnel than in flight. This may be attributed mostly to the mismatch in sensor location between tunnel and inflight units.

Figure 30 shows results of the wet conditions for Scoops 1 and 3 from Table 4. The comparison is consistently good between the tunnel and the different flight conditions considering the variability in the flight data itself. The same comments apply to the flange temperature TC1 and TC5 as discussed in the dry case comparisons. Overall comparison between the tunnel data and inflight data shows a very good agreement. Additionally, no ice or frozen runback was found to accrete on or downstream of the scoop surfaces in flight. Consequently, the design based on the tunnel data is validated.

Table 5 shows the conditions corresponding to dry and wet conditions for Scoop 2. In the dry conditions, inflight ambient temperatures were within 3 °C of the tunnel test conditions of Run 57 prior to activating the spray system. The comparison between the different dry flight conditions and Run 57 is shown in Figure 31. Generally speaking, the agreement is very good between the flight and the tunnel data. The first thermocouple represents the temperature near the scoop flange at the base of the scoop buttress. . There is some difference at the flange (TC1) and one of the downstream heaters (TC5). These differences could be due to differences in positioning of the sensors. The heater area corresponding to TC5 is large and the tunnel data model had two sensors (1 thermocouple and 1 RTD), which may not exactly correspond to the same location of TC5 on the flight unit. Nonetheless, the comparison is acceptable. Note that the flange temperature is less than 40 °C, which is well within the limit of 90 °C. This is typical of forward flight conditions.

Figure 32 shows comparisons for Scoop 2 in wet conditions. Here, the flight OAT is within 2 °C of the tunnel case. The LWC is high in all conditions and relatively close to the tunnel value with the exception of Flight condition 687b, which is 0.6 compared to 0.87 g/m^3 tunnel value. However, Figure 32 shows that thermocouple data from that flight are a little colder than the other flights despite their being at a slightly warmer OAT and lower LWC. This indicates that there are some variations and uncertainties in the flight data. The tunnel data in Figure 32 seems to be within this variability, which indicates very good correlation with flight data.

7.0 CONCLUDING REMARKS

A well-planned program was thoroughly executed to design an evaporative anti-icing system for the GKN WHL EH101 helicopter engine cooling bay inlet scoops.

Development of the anti-icing system was primarily based on icing tunnel tests. Although detailed CFD computations were conducted to study surface heat transfer and local flow characteristics, they were not reported in this paper. A final design was incorporated into flight test units based on the tunnel data. Very good agreement was obtained between flight, tunnel, and theoretical data.

Prior to the heater development tests, aerodynamic and ice shape evaluation tests were conducted to verify the icing tunnel setups based on prior flight test information that was crucial for Scoop 2. This required proper tunnel test fixture setups to yield equivalent flight effects. The use of isolated full-scale aircraft fairings in the vicinity of the component in consideration is not necessarily the correct approach, even in larger tunnels. Manipulation of spray nozzle locations and flow angularity with a simple airfoil reproduced the actual flight conditions.

Ice buildup on the forward facing step of the flange was associated with the turbulence effects that are common in icing tunnels. Flight video verified that this buildup was nonexistent in natural icing conditions. Nonetheless, this proves that development of an ice protection system in an icing wind tunnel yields a conservative design.

8.0 REFERENCES

[1]Al-Khalil, K., Salamon, L., and Tenison, G., “Development of The Cox Icing Research Facility,” AIAA 36th Aerospace Sciences Meeting, Reno, NV, Jan 1998, AIAA Paper 98-0097.

[2]Al-Khalil, K.M., "Effect of Mixed Icing Conditions on Thermal Ice Protection Systems," FAA Specialists' Workshop on Mixed-Phase and Glaciated Icing Conditions, Atlantic City NJ, Dec. 2-3, 1998.

ACKNOWLEDGMENTS

Permission to use the preceding results and the support of this program by the GKN Westland Helicopter company is acknowledged and appreciated. The success of this program is a result of the dedication and the team effort of several individuals within Cox & Company, Inc.

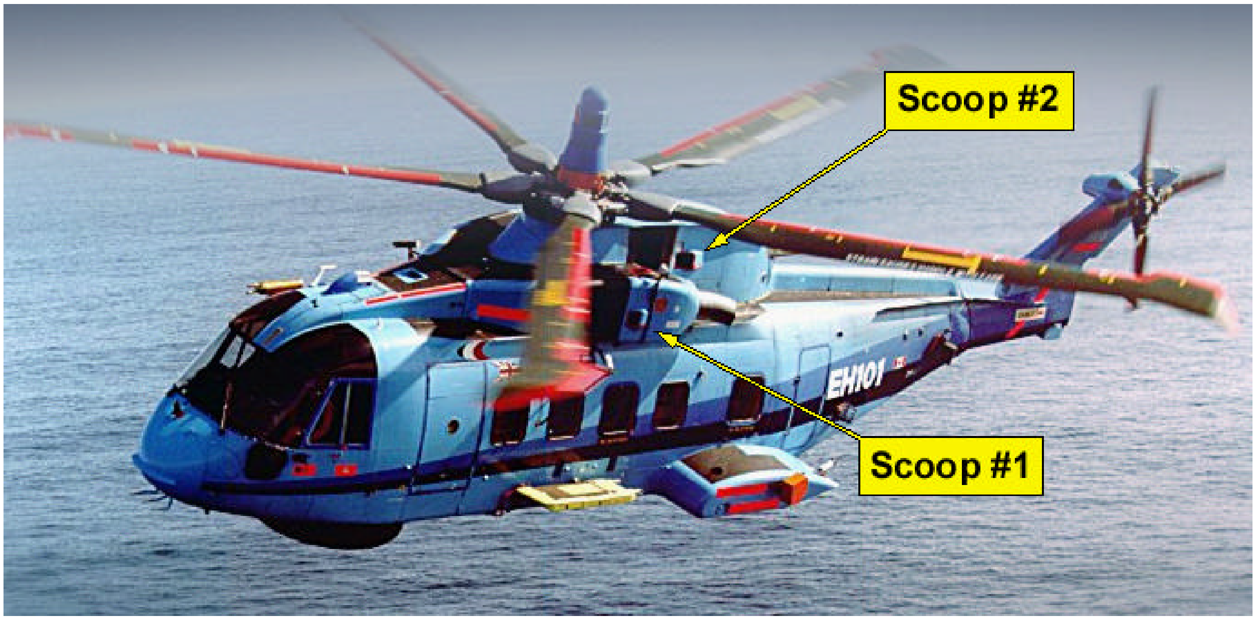

Figure 1: Location of Scoops on the GKN Westland Helicopter (EH101)
(Scoop 3 is symmetric to Scoop 1 on Starboard side)

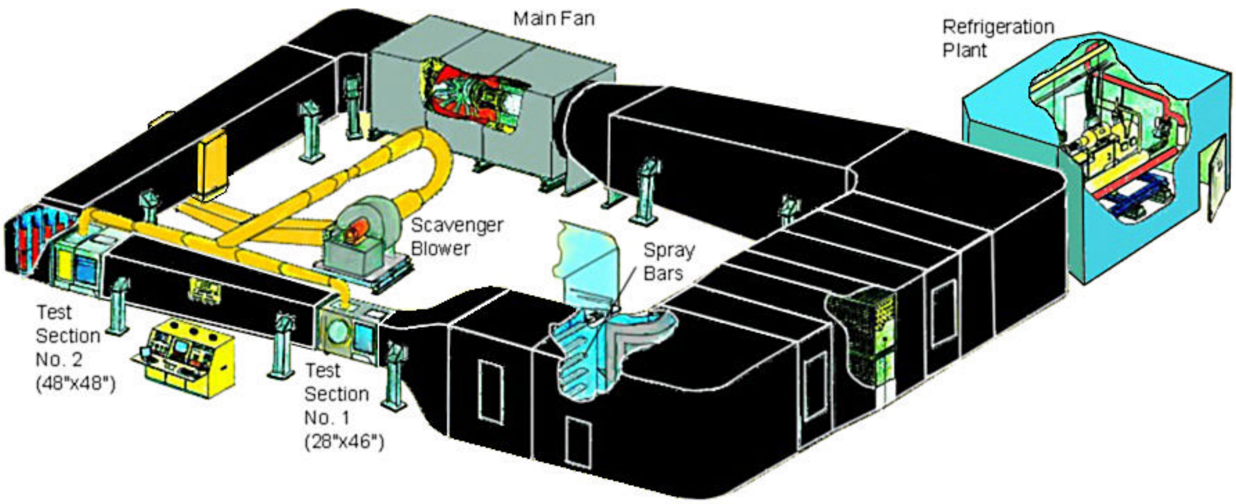

Figure 2: Layout of the IWT at the Cox LeClerc Icing Research Laboratory

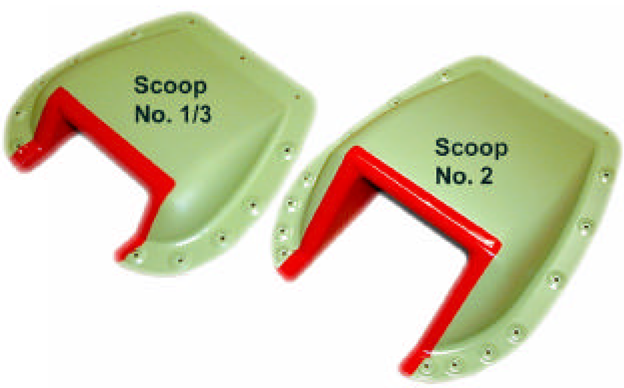

Figure 3: Engine cooling bay Scoops 1/3 and Scoop 2 on the GKN WHL EH101 Helicopter

Figure 4: Scoop 1 tunnel setup in Test Section-2

Figure 5: Cloud uniformity verification for Scoop 1 test setup

Figure 6: Glaze ice during flight on an earlier version of Scoop 1 (Flight 266)

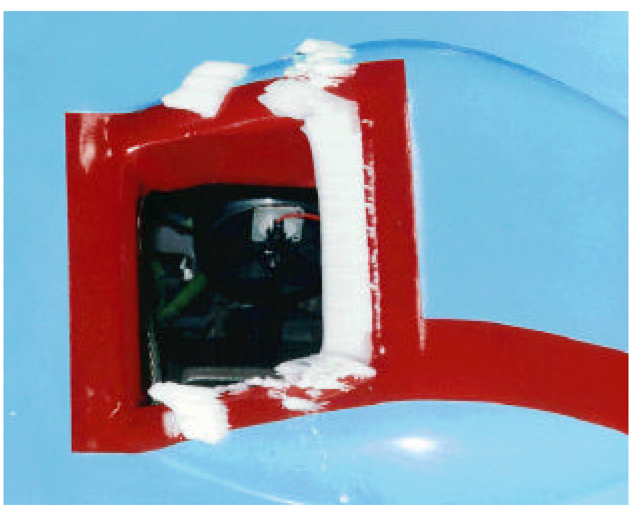

Figure 7: Rime ice during flight on an earlier version of Scoop 1 (Flight 257)

Figure 8: Glaze ice accretion and setup acceptance test for Scoop 1

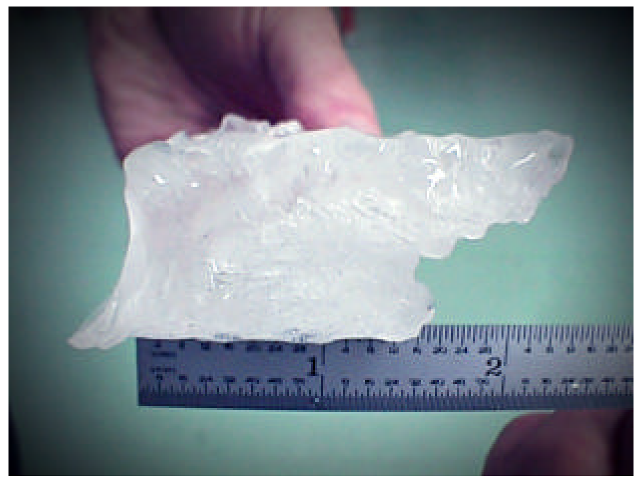

Figure 9: Glaze ice accretion for test setup verification of Scoop 1

Figure 10: Rime ice accretion and setup acceptance test for Scoop 1

Figure 11: Glaze ice during flight on Scoop 2 (Flight 266)

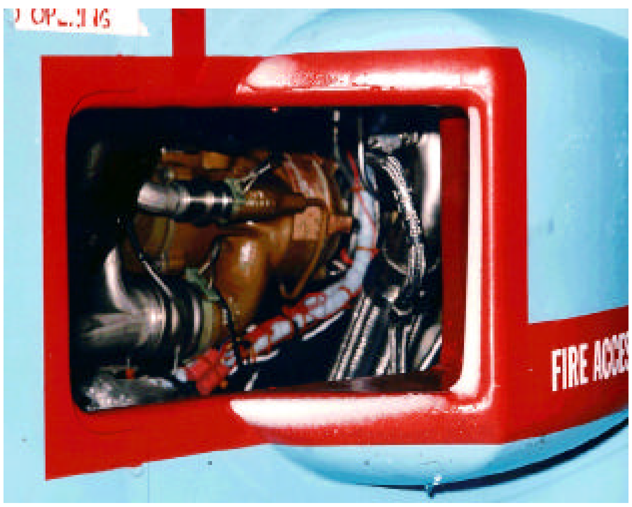

Figure 12: Rime ice during flight on Scoop 2 (Flight 257)

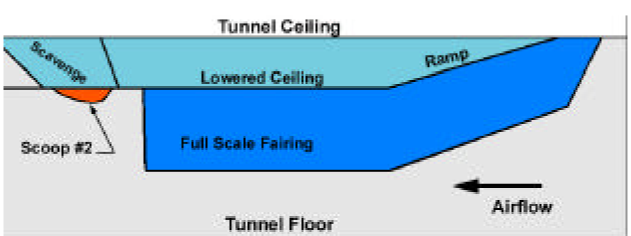

Figure 13: Side view of Scoop 2 tunnel setup with full scale fairing

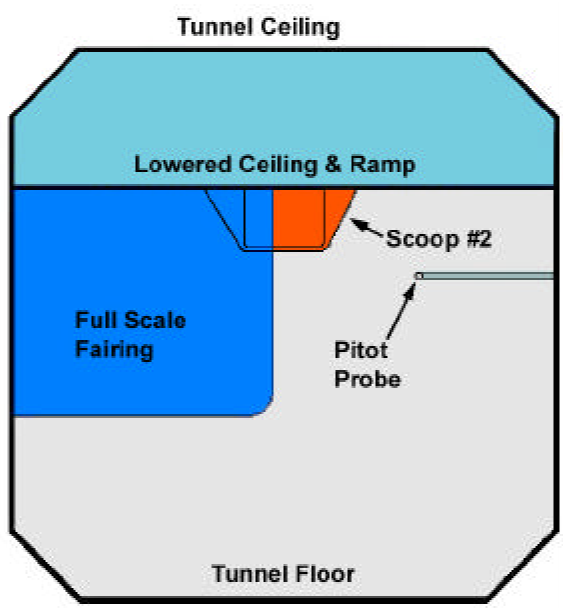

Figure 14: Downstream cross-section view near Scoop 2 with full scale fairing

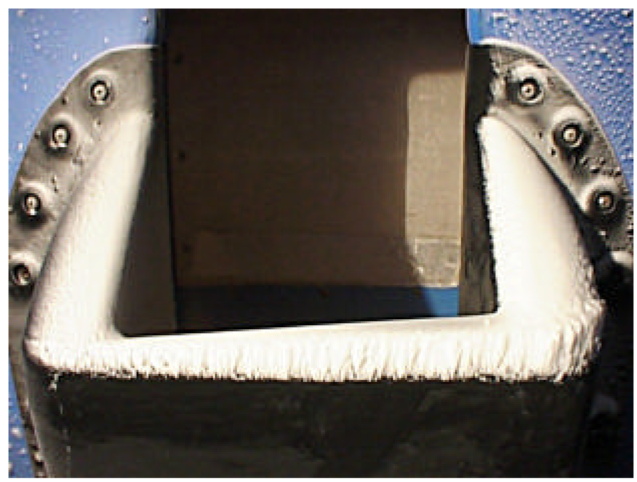

Figure 15: Rime ice on Scoop 2 with full size fairing (opposite effects seen in flight)

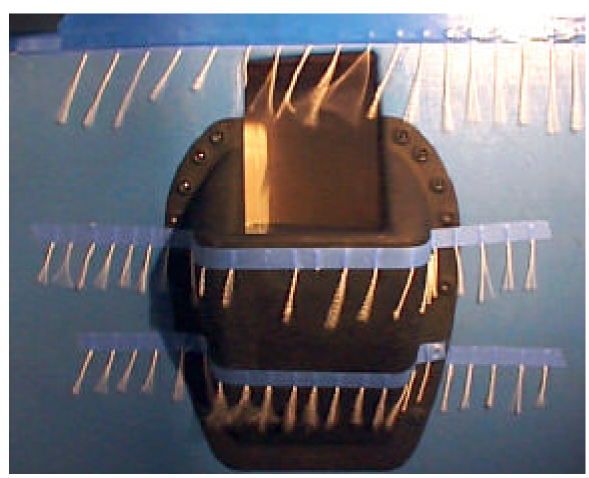

Figure 16: Flow visualization for Scoop 2 with full fairing setup

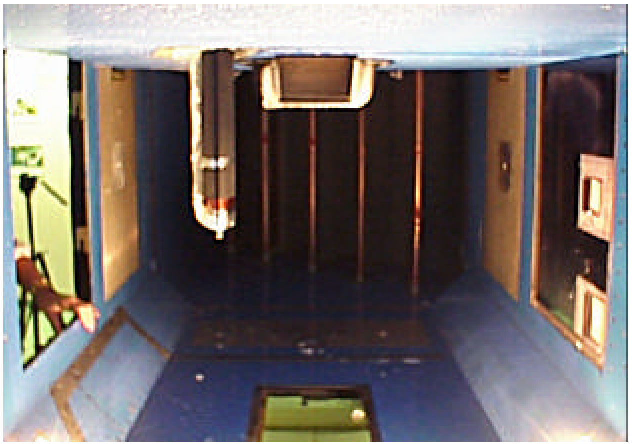

Figure 17: Downstream view of tunnel setup for Scoop 2 with airfoil flow deflector

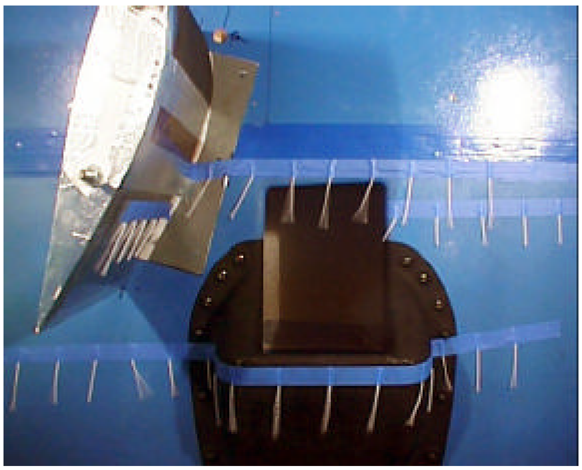

Figure 18: Flow visualization for Scoop 2 with airfoil flow deflector setup

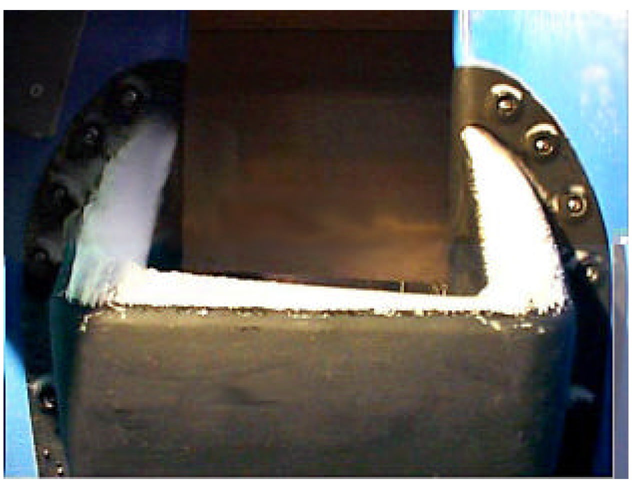

Figure 19: Rime ice on Scoop 2 with airfoil flow deflector (similar effects seen in flight)

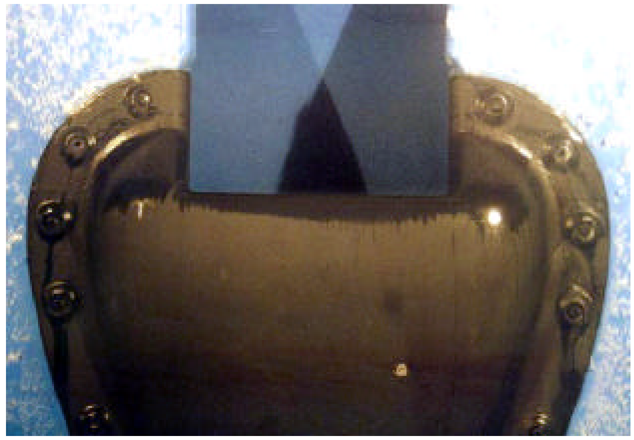

Figure 20: IPS performance in glaze icing conditions (Scoop 1)

Figure 21: IPS performance in rime icing conditions (Scoop 1)

Figure 22: IPS performance during rime and low speed conditions (Scoop 1)

Figure 23: IPS performance during alternate continuous and periodic maximum conditions (Scoop 1)

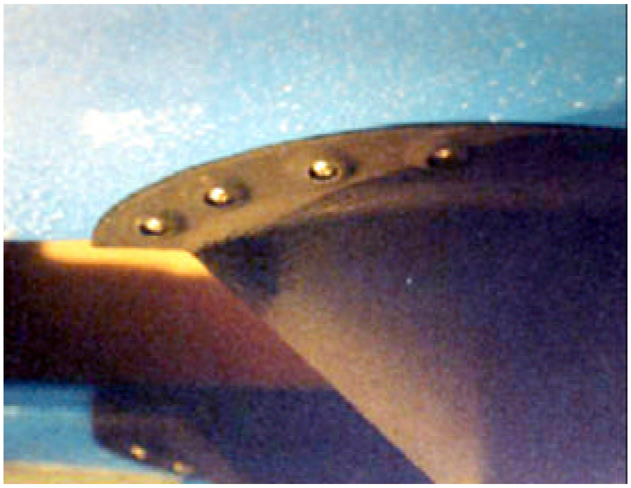

Figure 26: IPS performance during warm Intermittent Max conditions (Scoop 2)

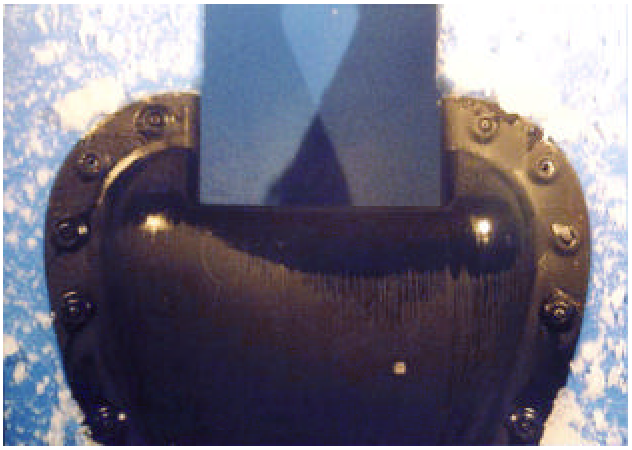

Figure 24: Evaporating runback in large droplet conditions (Scoop 1)

Figure 27: IPS performance during low speed Intermittent Max conditions (Scoop 2)

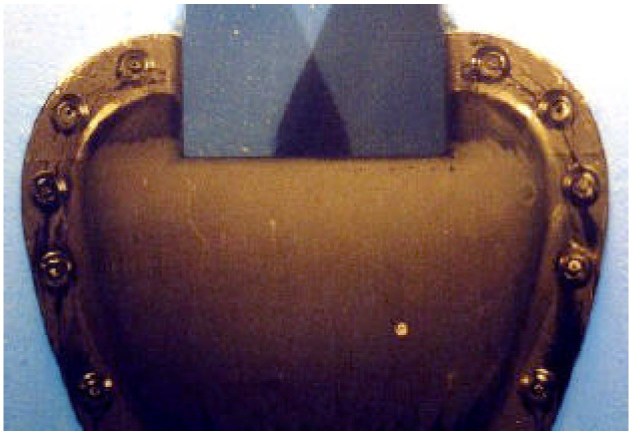

Figure 25: IPS performance during Intermittent Max conditions (Scoop 1)

Figure 28: IPS performance during very cold Intermittent Max conditions (Scoop 2)

Table 4: Tunnel and flight data comparison Conditions for Scoops 1 and 3

SCOOPS 1 & 3	Flight & Run No.	TIME hr:min	OAT (°F)	OAT (°C)	V (KTAS)	LWC (g/m^3)
DRY	FLT 689	20:00	21	-6.1	120	0
	FLT 687a	15:00	32	0.0	120	0
	FLT 700	18:31	32	0.0	120	0
	RUN 21		26	-3.3	120	0
WET-1	FLT 687b	16:12	30	-1.1	120	0.6
	FLT 698	15:57	28	-2.2	120	0.6
	FLT 712b	18:37	28	-2.2	120	0.6
	RUN 21		26	-3.3	120	0.57

Table 5: Tunnel and flight data comparison Conditions for Scoop 2

SCOOP 2	Flight & Run No.	TIME hr:min	OAT (°F)	OAT (°C)	V (KTAS)	LWC (g/m^3)
DRY	FLT 689	20:00	21	-6.1	120	0
	FLT 687a	15:00	32	0.0	120	0
	FLT 700	18:31	32	0.0	120	0
	RUN 57		26	-3.3	120	0
WET	FLT 687b	16:12	30	-1.1	120	0.6
	FLT 712a	18:10	27	-2.8	120	0.9
	FLT 712c	17:17	28	-2.2	120	1
	RUN 57		26	-3.3	120	0.87

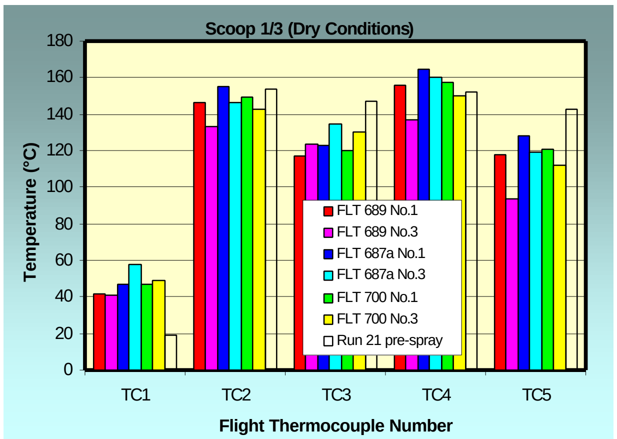

Figure 29: Tunnel and flight data comparison for Scoops 1 & 3 in dry air

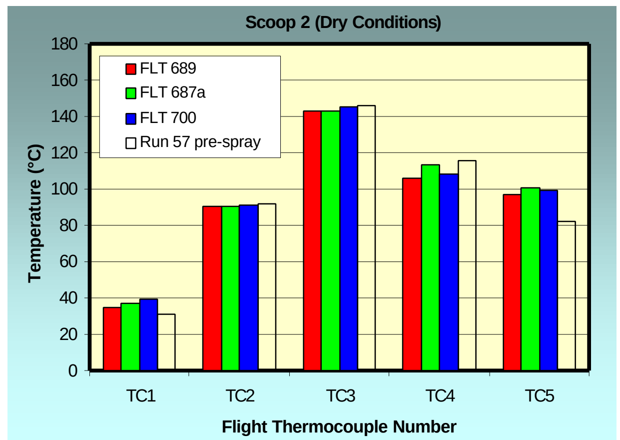

Figure 31: Tunnel and flight data comparison for Scoop 2 in dry air

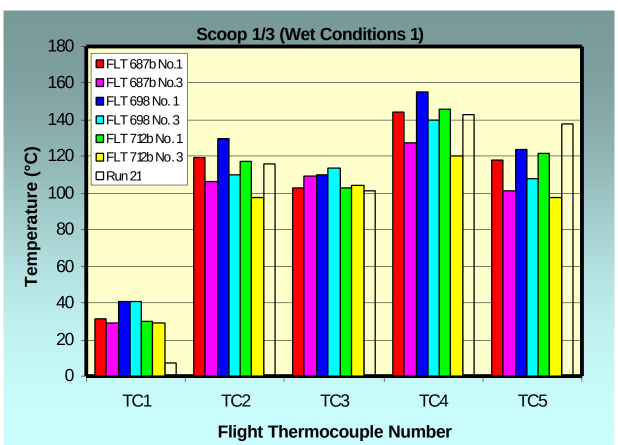

Figure 30: Tunnel and flight data comparison for Scoops 1 & 3 in wet conditions

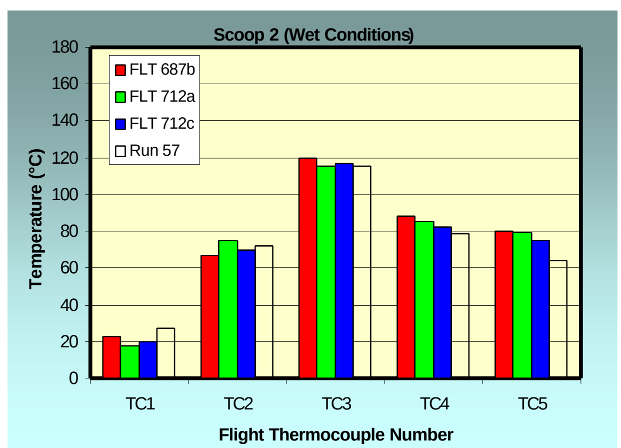

Figure 32: Tunnel and flight data comparison for Scoop 2 in wet conditions